Organic & Biomolecular Chemistry

Cite this: *Org. Biomol. Chem.*, 2012, **10**, 5332

www.rsc.org/obc

**PERSPECTIVE**

# Self-assembly driven by an aromatic primary amide motif

**Myungeun Seo,† Jeyoung Park and Sang Youl Kim***

***Received 15th January 2012, Accepted 3rd April 2012***
**DOI: 10.1039/c2ob25117e**



Primary amides are unique supramolecular synthons possessing two hydrogen donors and two hydrogen acceptors. By interacting in a complementary fashion, primary amides reliably generate two-dimensional hydrogen bonded networks that differ from conventional hydrogen bonded structures such as carboxylic acid dimers or one-dimensional secondary amide chains. This feature permits the design of sophisticated supramolecular assemblies based on primary amides (especially aromatic amides). Several interesting crystal structures have been constructed utilizing primary amides, although such structures have been applied only in the field of crystal engineering because the networks strongly favor crystallization. Expansion of the applications of primary amides to liquid crystals and self-assembly in solution requires an appropriate balance between primary amide-based hydrogen bonding and other noncovalent interactions. This perspective article reviews the key hydrogen bonding properties of primary amides determined from crystal structure studies, and a variety of supramolecular assemblies involving primary amides are discussed. A new strategy for overcoming crystallinity and solubility issues is proposed, involving introduction of a trifluoromethyl group at the *ortho* position of the aromatic primary amide. Such substitutions produce highly processable primary amides, while maintaining the two-dimensional hydrogen bonded network. Examples of self-assembly using 2-trifluoromethylbenzamide demonstrate its usefulness in self-assembly.

## Introduction

Hydrogen bonding is one of the most important noncovalent interactions in the context of self-assembly. It is the most reliable element for the construction of assemblies of neutral molecules because hydrogen bonds are highly directional and their interaction strengths can be tuned by the choice of the donor–acceptor pair. The N–H···O═C hydrogen bond in an amide

*Department of Chemistry, Korea Advanced Institute of Science and Technology (KAIST), 373-1, Guseong-dong, Yuseong-gu, Daejeon, 305- x701, Korea. E-mail: kimsy@kaist.ac.kr; Fax: (+82) 42-350-8177; Tel: (+82) 42-350-2834*

†Current address: Department of Chemistry, University of Minnesota, Minneapolis, MN, 55455-0431, USA.

**Myungeun Seo**

*Dr Myungeun Seo received his Ph.D. in 2008 from the Department of Chemistry at KAIST (South Korea) under the supervision of Prof. Kim, on self-assembly of benzamide-containing molecules. After spending one year as a postdoctoral fellow in the same group, he moved to Prof. Marc A. Hillmyer's group at the University of Minnesota and is currently working on block copolymer based nanoporous materials. His research interests focus on self-assembled organic nanostructures.*

**Jeyoung Park**

*Mr Jeyoung Park received his M.S. in 2008 from the Department of Chemistry at KAIST (South Korea) under the supervision of Prof. Kim. He stayed in Prof. Kim's lab and is now pursuing his Ph.D. degree. His research interests include controlled synthesis and self-assembly of polymers.*

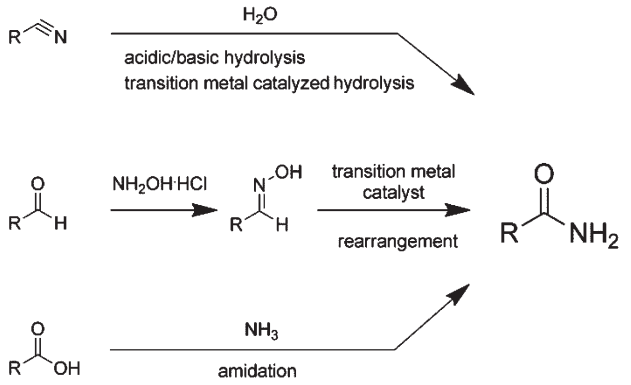


**Scheme 1** Synthetic routes to primary amides.

motif, for instance, has an N–H donor and C═O acceptor, which provide a particularly strong and directional self-complementary hydrogen bond.[1] Thus, it is not surprising that hydrogen bonding between amides plays a crucial role in biological molecules and forms the basis for a variety of complex self-assembled nanostructures.[2]

## Primary amides

Of particular interest in this article are primary amides (carboxamides), which have the formula O═C–$NH_2$. Primary amides are common motifs in natural products and pharmaceuticals due to their biological relevance. They are also important functional groups in synthetic organic chemistry as intermediates and raw materials. Scheme 1 illustrates the various synthetic routes to producing primary amides. Primary amides are usually synthesized *via* the hydration of nitriles by either acid or base catalysis;[3] however, disadvantages, such as the harsh reaction conditions, potential production of acids as a side product, and the challenges associated with preparing compounds containing more than two nitrile groups have been recognized.[4] The selective conversion of nitriles to amides has been performed using transition metal complexes.[5–7] Recently, the more atom-efficient conversions of aldoximes or aldehydes into primary amides have attracted synthetic interest.[8–10] Another conventional method for preparing primary amides is the reaction of activated carboxylic acid derivatives with ammonia or urea.[11,12] Recent reports describing synthetic approaches to primary amides have been summarized elsewhere.[11,13–15]

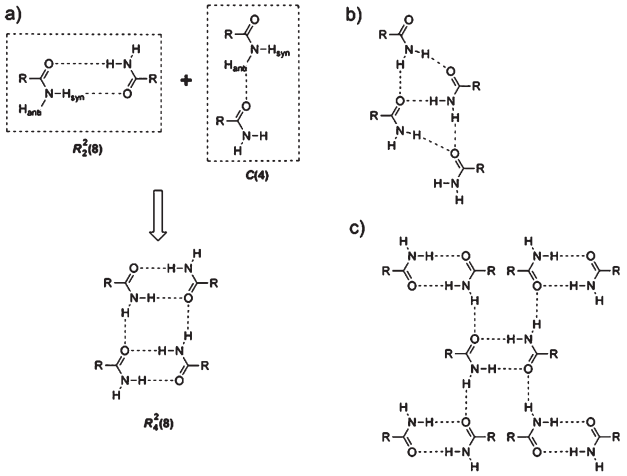


**Fig. 1** Two-dimensional hydrogen bonded networks of primary amides. (a) Construction of 5 Å translation motif ($R_4^2(8)$ network) by graph set notation. (b) $2_1$ axis motif. (c) Glide motif.

Primary amides provide unique motifs in self-assembly because of their ability to form two-dimensional hydrogen bonded networks. Tertiary amides (O═C–$NR_2$) act as hydrogen bond acceptors only (thus they cannot form self-complementary hydrogen bonds), and secondary amides (O═C–NH–R) provide only one type of hydrogen bond; however, primary amides can form hydrogen bonds in two directions thanks to the presence of two hydrogen atoms connected to each nitrogen atom. In graph set notation, hydrogen bonding patterns of primary amides can be described as a combination of two supramolecular synthons: a cyclic dimer $R_2^2(8)$ utilizing a *syn*-oriented hydrogen atom ($H_{syn}$) to form face-to-face hydrogen bonds, and a chain $C(4)$ utilizing an *anti*-oriented hydrogen atom ($H_{anti}$) to form side-to-side hydrogen bonds. This yields a two-dimensionally extended ladder-type network $R_4^2(8)$ (Fig. 1a).[1,16]

Hydrogen bonding patterns of primary amides in molecular crystals have been extensively studied by Leiserowitz and Schmidt.[17] In the crystal structures of molecules containing a primary amide, centrosymmetric dimers $R_2^2(8)$ are reliably produced and usually display an O···H distance of 2 Å.[18,19] If centrosymmetric dimers form, successive pairs are usually related by a 5 Å translation and form a network of $R_4^2(8)$ elements.[1] Other structures, such as the $2_1$ axis motif (Fig. 1b) and the glide motif (Fig. 1c), have been identified. Whereas a 5 Å translation is generally favored over other structures, the structure depends on the R-group connected to the amide.[19] For example, cubanecarboxamides adopt a shallow glide packing structure to reduce steric hindrance among the bulky cubyl groups (5.4 Å).[1] Although dimer formation of primary amides through face-to-face hydrogen bonding of N–$H_{syn}$···O is highly stable, $H_{anti}$ can form hydrogen bonds with other hydrogen bond acceptors under competing conditions.[20] For example, the bulky triphenylmethyl group in 4-tritylbenzamide can force $H_{anti}$ to find acceptors other than carbonyl oxygen atoms in benzamide, leading to formation

**Sang Youl Kim**

*Professor Sang Youl Kim received his Ph.D. in 1989 from Rensselaer Polytechnic Institute (USA). Now he is a professor in the Department of Chemistry at KAIST (South Korea). His research interests include self-assembled organic materials, functional macromolecules, controlled polymerization, and advanced polyolefin materials.*

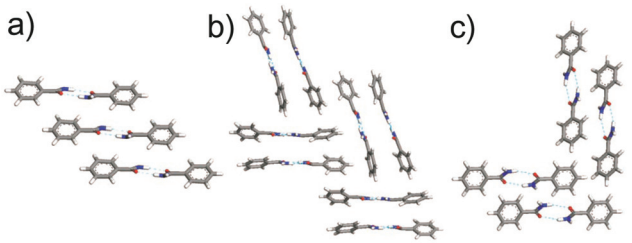


**Fig. 2** Polymorphism in benzamide. (a) Shifted stacks, view along [010]. (b) Herringbones, view along [001]. (c) T-shaped, view along [100]. Reprinted from ref. 24 with permission from Wiley-VCH.



of N–H···O═C hydrogen bonds with solvent molecules possessing carbonyl groups.[21] Crystallization of the host in an aromatic solvent leads to an $H_{anti}$ bonded to one of the phenyl rings in the triphenylmethyl group *via* an N–H···π interaction.

### Self-assembled molecular crystals based on primary amides

The hydrogen bonding properties of primary amides have been used to prepare interesting molecular crystals, for example, crystals based on aromatic primary amides (benzamides). It should be noted that the crystal structure of benzamide itself is complicated due to the existence of several polymorphic forms. Actually, benzamide is famous as the first identified example of a polymorphic crystalline compound, discovered in 1832.[22] Recently, two additional polymorphic forms were identified.[23,24] Two-dimensional hydrogen bonded networks related by translations are conserved in polymorphic forms, reflecting the fidelity of the hydrogen bonds of primary amides. In contrast, π–π interactions among phenyl rings induce the formation of polymorphs with different packing structures (shifted stacks, herringbones, or T-shaped), as shown in Fig. 2.[24] These results suggest that in addition to primary amides, other parts of a molecule should be considered in the design of self-assembled structures so as to achieve an appropriate balance in the directionality of noncovalent interactions.

Aromatic primary amides have been introduced into complex molecular structures to form molecular crystals. The introduction of four aromatic primary amides to the periphery of a tetrakisporphyrin yielded a two-dimensional open network structure based on the amide hydrogen bonds.[25] The network contained interporphyrin cavities filled with solvent (dimethylsulfoxide, DMSO), which may potentially be used as functional nanopores (Fig. 3a). Other functional two-dimensional networks consisting of *o*-bis(amide)-appended ethylenedithiotetrathiafulvalene have been prepared.[26] The presence of two adjacent amide motifs enabled the formation of a "hydrogen bonded ribbon" structure based on radical cation salts (with counter anions) that provided good conductivity (Fig. 3b). A three-dimensional hydrogen bonded network was obtained from 2,2′,5,5′-substituted biphenyl units with intralayer face-to-face hydrogen bonds and interlayer side-to-side hydrogen bonds (Fig. 3c).[27] Another interesting three-dimensional network was derived from hexakis(4-carbamoylphenyl)benzene, which showed solvent-induced polymorphisms (Fig. 3d).[28] Crystallization of the compound in DMSO yielded a porous network filled with solvent and connected *via* side-to-side hydrogen bonding. The strongest hydrogen bond donor in the system, $N–H_{syn}$ in the primary amide, bonded to the strongest acceptor, S═O in DMSO, to form a porous structure. A propanol (*n*-PrOH)–water mixture induced formation of a different crystalline porous network solvated by propanol, which formed hydrogen bonds between the weak hydrogen bond accepting propanol oxygen and the $N–H_{anti}$ in the primary amide. Growth of the crystals under hydrothermal conditions favored the more hydrophobic and π–π interactions, which yielded a nonporous crystal.

Two-dimensional crystallization on the surfaces of aromatic primary amide-containing molecules was investigated by Matzger and coworkers (Fig. 4).[29] 4-Alkyloxybenzamides with alkyl chains 12–18 carbons long formed nanoporous rhombic crystalline lattices at the 1-phenyloctane/highly oriented pyrolytic graphite (HOPG) interface. This structure was unusual, considering the symmetry of the molecule. A 6-fold rotational symmetry was noticed from six bifurcated hydrogen bonds, where both the hydrogen atoms connected to the nitrogen equally pointed to the neighboring carbonyl oxygen. The nanoporous structure was solely formed from 4-dodecyloxybenzamide; however, other phases, such as a close-packed structure, were observed for longer alkyl chains, indicating that the rhombic phase did not result from the alignment of the alkyl chain with the substrate surface. A carboxylic acid analog only produced a close-packed structure, indicating the importance of the hydrogen bonding of benzamides. The driving force for overcoming the large stability difference between the close-packed structures and the nanoporous structures was attributed to epitaxial stabilization by HOPG, solvent coadsorption in voids, and equilibrium adsorption and desorption in solution.[30]

### Self-assembly based on primary amides: beyond crystals

During the fabrication of other types of self-assembled materials, such as liquid crystals, primary amide motifs are rarely as useful as secondary amides or carboxylic acids. The tendency of primary amides to form two-dimensional hydrogen bonded networks increases the propensity for crystallization, which is unsuitable for self-assembly. Tschierske and coworkers performed an interesting study that explored this relationship. They studied several functional groups at the lateral (2′) position of the *p*-terphenyl unit (Fig. 5).[31] The primary amide derivative remained crystalline up to 184 °C (the second highest melting temperature in the series after the sodium carboxylate derivative) and became isotropic above this temperature, whereas the methyl ester, carboxylic acid, and hydrazine derivatives showed nematic or smectic A phases. The propensity of the primary amides to form crystals was demonstrated in a study of hydrazine-based low molecular weight organic gelator (4-alkyloxybenzohydrazide) derivatives, in which the benzamide analog (4-dodecyloxybenzamide in Fig. 4) did not form a gel in solvents.[32]

The tendency of primary amides to form crystals could be overcome by introducing a primary amide group at the focal point of a dendron, which acted as a large wedge-shaped building block that drove self-assembly *via* dendron packing. Dendrons formed from rigid scaffolds and flexible peripheral chains displayed liquid crystalline behavior based on microphase separation between the scaffold and chain.[33] An early example of introducing a bulky counterpart into a primary amide was

 

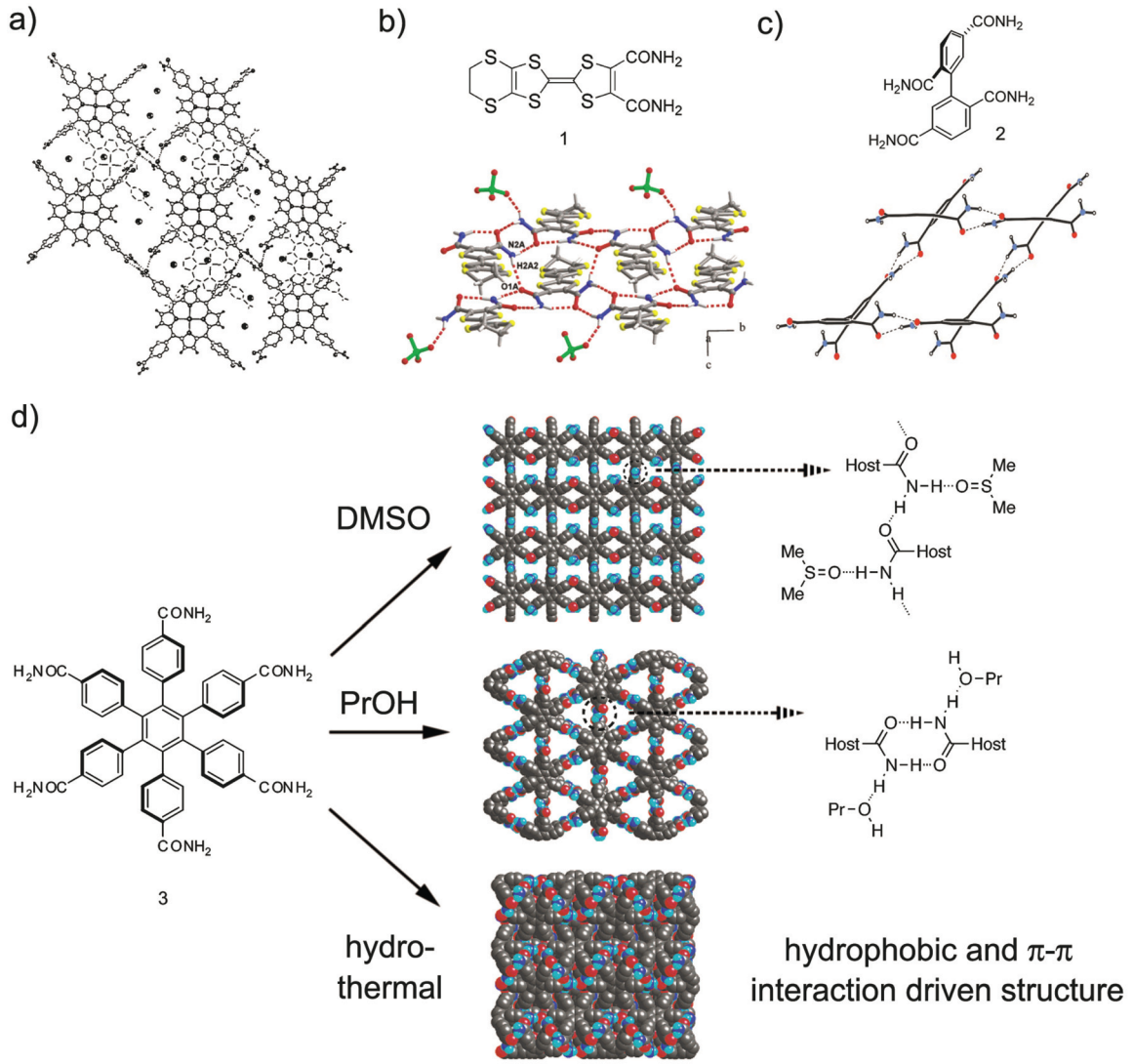


**Fig. 3** Introduction of aromatic primary amides to molecular crystals. (a) Two-dimensional open networks of zinc tetra(4-amidophenyl)porphyrin. Each of the interporphyrin cavities was occupied by two molecules of DMSO, as indicated by the large darkened circles. Reprinted from ref. 25 with permission from Royal Society of Chemistry. (b) The chemical structure of *o*-bis(amide)-appended ethylenedithiotetrathiafulvalene **1**, a corresponding perspective view into the hydrogen bonded ribbon, and the interribbon pattern formed by $\mathbf{1}_2ClO_4$. Reprinted from ref. 26 with permission from American Chemical Society. (c) Chemical structure of 1,1′-biphenyl-2,2′,5,5′-tetracarboxamide **2** and the corresponding crystal formed by intermolecular double hydrogen bonds. Reprinted from ref. 27 with permission from Elsevier Inc. (d) Chemical structure of hexakis(4-carbamoylphenyl)benzene **3** and the corresponding 3D hydrogen bonded networks of **3**·12DMSO (top), **3**·6*n*-PrOH (middle), and **3**·$H_2O$ (bottom). Carbon, nitrogen, oxygen, and hydrogen atoms are shown in gray, blue, red, and light blue, respectively. Solvent molecules are omitted for clarity. Hydrogen bonding patterns of **3** with DMSO and with *n*-PrOH are also shown. Reprinted from ref. 28 with permission from American Chemical Society.

provided by the 3,4,5-trisalkoxybenzamides ("three-chain" benzamides), which displayed liquid crystal mesophases of columnar or stack-like structures. The importance of the bulky alkoxy chains was noted by the fact that neither the 4-monoalkoxybenzamide nor 3,4-bisalkoxybenzamide displayed mesomorphism, whereas 3,5-bisoctyloxybenzamide displayed a mesophase identical to that of the 3,4,5-trisalkoxy analogs. Hydrogen bonding between benzamides was important because it stabilized the column structures; benzoic acid or the *N*-methylated analogs failed to produce a mesophase.[34]

Percec *et al.* synthesized hybrid dendrons with benzyl ether or biphenyl methyl ether repeating units and a variety of functionalities, including benzamides, at the focal points (Fig. 6a, for example).[35] Appropriate selection of the dendron scaffold resulted in formation of porous columns regardless of the functional groups at the focal points. This indicated that the self-assembly process was dominated by the dendrons rather than the functionality at the focal point. The focal point, therefore, provides an opportunity for introducing a variety of functionalities into the self-assembled structure. Aromatic primary amides were introduced at the focal points of a stilbenoid dendron (Fig. 6b) along with other functional groups.[36] The electronic properties of the dendron were governed by the stilbenoid scaffold, and the focal functional group did not significantly

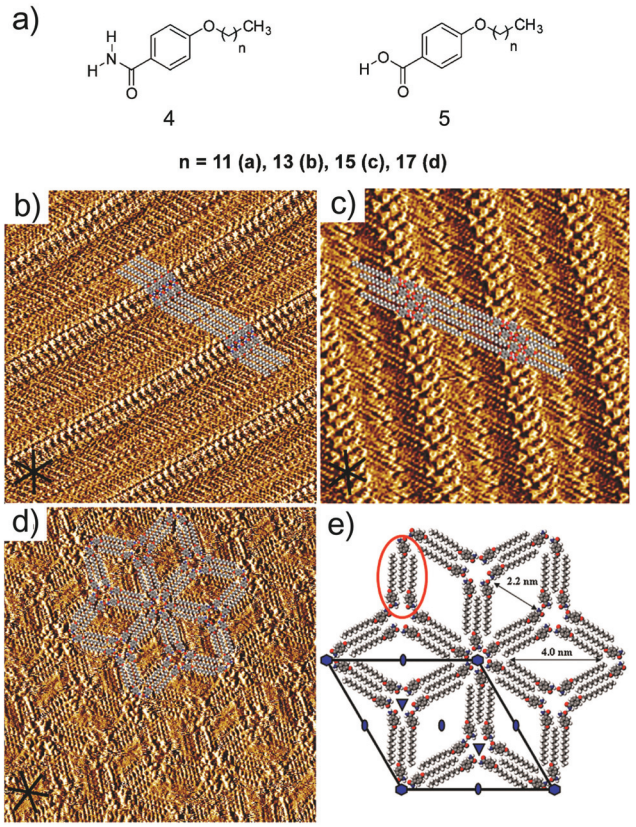


**Fig. 4** Crystallization of aromatic primary amides on the surface. (a) Chemical structures of 4-alkyloxybenzamide **4** and 4-alkyloxybenzoic acid **5**. Scanning tunneling microscopy (STM) images formed at the 1-phenyloctane/HOPG interface and the computed models of (b) **4d**, (c) **5d**, and (d) **4a** (20 × 20 $nm^2$). (e) A computed model of Fig. 4d with a unit cell. The black axes indicate the symmetry of HOPG under the monolayer. The red oval indicates an asymmetric unit of the rhombic nanoporous network. Reprinted from ref. 29 with permission from American Chemical Society.

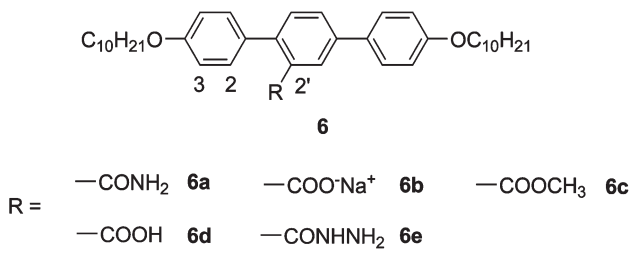


**Fig. 5** Chemical structures of calamitic mesogens containing *p*-terphenyl derivatives functionalized at the lateral (2′) position. Reprinted from ref. 31 with permission from Royal Society of Chemistry.

affect the electronic properties. All other derivatives prepared in the study formed hexagonal columnar liquid crystalline phases; however, the primary amide derivative formed a cubic phase at elevated temperatures. FT-IR spectroscopy revealed a red shift in the N–H stretching vibration, which suggested that most of the amides participated in hydrogen bonding. Thus, the phase behavior was attributed to hydrogen bonding among the aromatic primary amides.

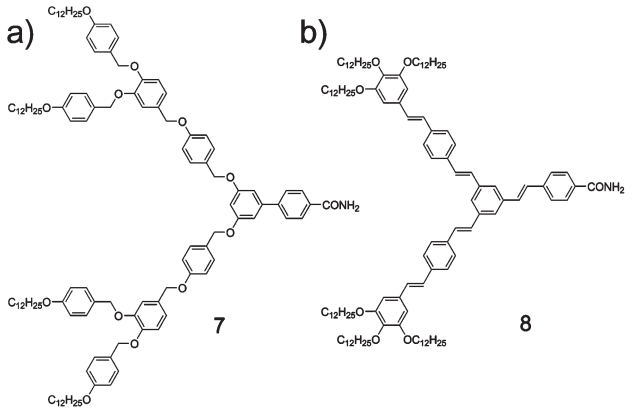


**Fig. 6** Chemical structures of (a) hybrid dendron comprising benzyl ether and biphenyl methyl ether repeating units (reprinted from ref. 35 with permission from Wiley-VCH) and (b) stilbenoid dendron (reprinted from ref. 36 with permission from Royal Society of Chemistry), in which aromatic primary amides were introduced at the focal points.

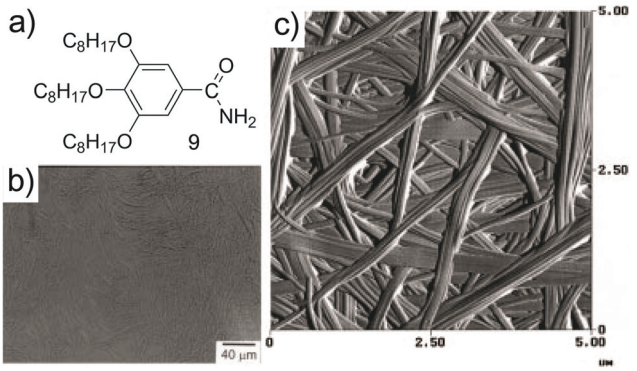


**Fig. 7** Self-assembly of aromatic primary amides in solution. (a) Chemical structure of 3,4,5-tris(octyloxy)benzamide **9**. (b) Polarized optical image and (c) SFM image of the xerogel of **9** from styrene. Reprinted from ref. 40 with permission from Wiley-VCH.

### Self-assembly in solution

The association constants of primary amides in benzene or 1,4-dioxane solutions were determined by Bates and Hobbs through measurements of the dipole moments of the solutions. The authors concluded that a highly polar enolic tautomer form did not contribute to the structure of the amide.[37] Association occurred in the nonpolar benzene solution but not in 1,4-dioxane. Because the measurements were performed at low concentrations, dimerization was assumed, and association constants were obtained in the range 40–300 $M^{-1}$. *m*-Substituted benzamides showed the highest association constants among the molecules studied.[38] An IR study of primary amides suggested that they may associate into clusters larger than dimers at higher concentrations in $CCl_4$.[39]

The first recognition of self-assembly and the production of nanoscopic objects among primary amide-containing molecules in solution was performed using 3,4,5-tris(octyloxy)benzamide, which displays liquid crystalline properties, as discussed previously (Fig. 7a).[40] Physical gelation could be induced upon rapid cooling of a hot solution to −180 °C (1200 °C $min^{-1}$,

 

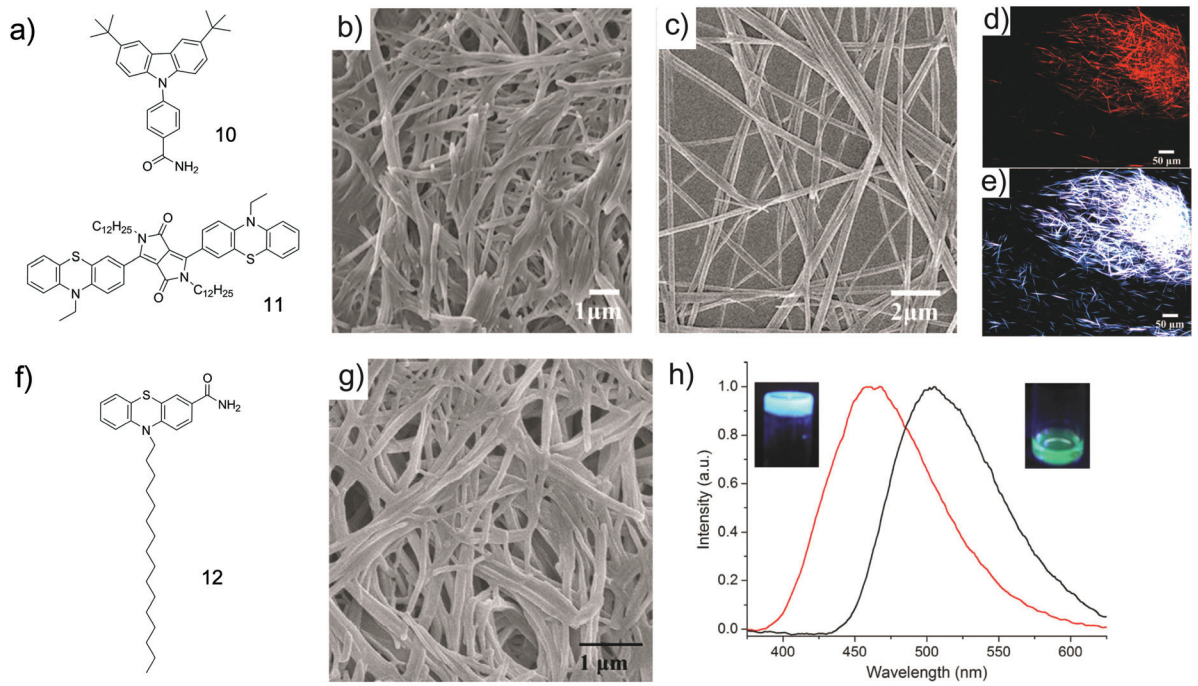


**Fig. 8** Self-assembly of aromatic primary amides in conjugated aromatics. (a) Chemical structures of the carbazole-based organogelator **10** and the diaryldiketopyrrolopyrrole derivative functionalized with phenothiazine moieties **11**. SEM images of (b) the xerogel of **10** and (c) the composite xerogel based on **10** and **11** (the molar ratio is 10 : 1) from cyclohexane. (d,e) Fluorescence microscopy images of the composite gel of Fig. 8c excited at (d) 510–550 nm or (e) 330–385 nm. Reprinted from ref. 43 with permission from American Chemical Society. (f) Chemical structure of phenothiazine-based organogelator **12**. (g) SEM image of the xerogel of **12** from ethanol–water (v/v = 5 : 1). (h) Normalized fluorescence spectra of **12** in solution (black line) and in gel (red line) in ethanol–water (v/v = 5 : 1), excited at 325 nm (right inset: optical image of a solution containing **12** at 80 °C, left inset: optical image of the gel of **12** at 25 °C, excited at 325 nm). Reprinted from ref. 44 with permission from Elsevier Inc.



"freeze shocking"). This method yielded a stable gel by suppressing crystallization in a variety of solvents, including alcohols, esters, methacrylates, amines, and aromatics at concentrations of 1–2.5 wt%. Long needle-like aggregates smaller than 1 μm in diameter were observed in the dried gel (Fig. 7b). Scanning force microscopy (SFM) revealed that each strand consisted of bundles of parallel fibers (Fig. 7c). This observation was consistent with the general mechanism of physical gelation in the presence of a low molecular weight gelator, which includes aggregation of small molecules into nanoscopic fibers and network formation by branching or entanglement.[41] The authors, however, did not investigate hydrogen bonding among the amides in the study. Because the compound formed gels from vinylic monomers, such as styrene or methyl methacrylate, gelation and photopolymerization of monomer and crosslinker mixtures enabled embedding of a self-assembled matrix in the polymer.

Introduction of a primary amide motif into conjugated aromatics in which π–π interactions play a significant role can provide another way to utilize primary amides in self-assembly. Lu *et al.* employed aromatic primary amides in the design of electroactive organogelators based on carbazole and phenothiazine units (Fig. 8). Carbazole-based organogelators bearing two *t*-butyl groups formed nanofibers several millimeters in length in cyclohexane, directed by balanced hydrogen bonding and π–π interactions.[42] The electron-rich compound was mixed with an electron-deficient diaryldiketopyrrolopyrrole derivative to investigate photoinduced energy transfer in the self-assembled state.[43] Scanning electron microscopy (SEM) and X-ray diffraction experiments showed that diaryldiketopyrrolopyrrole derivative was embedded in the self-assembled fibers. An FT-IR study indicated that the incorporation of diaryldiketopyrrolopyrrole disrupted hydrogen bonding among the primary amides to some extent; however, the self-assembled network structure was retained. The emission wavelength could be tuned by varying the excitation wavelength. Visible light excited only the diaryldiketopyrrolopyrrole and produced red emission; however, UV irradiation induced partial energy transfer from the carbazole to the diaryldiketopyrrolopyrrole and generated a purplish white color. Phenothiazine-based organogelators could produce a gel in a mixture of water and ethanol over a narrow compositional range to produce an aggregation-induced blue shift in the emission spectrum. This blue shift was attributed to the suppression of twisted intramolecular charge transfer due to the restricted rotation in the gel state.[44]

## 2-Substituted aromatic primary benzamides: 2-trifluoromethyl benzamide

We attempted to use an aromatic primary amide motif to form self-assembled molecular crystals as well as other types of self-assembled materials. Our approach included introduction of a substituent, the trifluoromethyl group, at the *ortho* position of

the aromatic primary amide. Rotation of exocyclic C–C bonds is strongly restricted in 2-substituted benzamides, and the carbonyl group usually points toward the substituent to reduce steric crowding due to hydrogen bonding.[45,46] However, the ability of $H_{anti}$ in the amide to form hydrogen bonds with other hydrogen bond acceptors must be considered in 2-substituted benzamides. Fluorine can interact with hydrogen to form F–H bonds, and an intramolecular F–H bond has been observed in crystals of $CF_3CFXCONH_2$, where X denotes another halogen.[47] 2-Trifluoromethylbenzamide was, therefore, of interest because the trifluoromethyl substituent (1) was sterically bulky and disturbed the π–π interactions among the aromatic rings, potentially improving the solubility; and (2) possessed fluorines that could compete with the carbonyl oxygen of the neighboring amide to form hydrogen bonds with $H_{anti}$. Thus, we sought to investigate the types of hydrogen bonding structures that could be produced in the 2-trifluoromethylbenzamide.

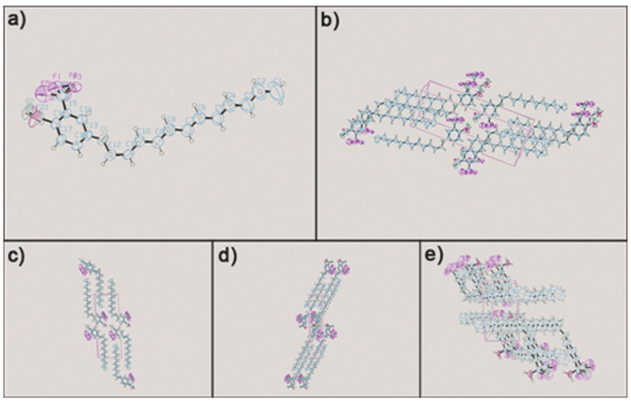


**Fig. 9** (a) Crystal structure of 4-dodecyloxy-2-trifluoromethylbenzamide obtained from hexane. (b) Crystal shows two kinds of hydrogen bonds. Projection on to (c) (100), (d) (101), and (e) (001) direction. Hydrogen, carbon, oxygen, nitrogen, and fluorine atoms are shown in black, blue, green, red, and purple, respectively.

### Molecular crystals: macroscopic parallelogrammatic pipes

An amphiphilic molecule was designed by combining 2-trifluoromethylbenzamide and an aliphatic alkyl chain through an ether linkage.[48] The ether linkage was formed by nucleophilic aromatic substitution ($S_NAr$) of 4-nitro-2-trifluoromethylbenzonitrile (nitro group as the leaving group) and 1-dodecanol. 4-Nitro-2-trifluoromethylbenzonitrile provided a key intermediate. An $S_NAr$ reaction with an alcohol was feasible in the presence of a strong electron-withdrawing nitrile and the trifluoromethyl groups, and basic hydrolysis of the nitrile group produced the desired benzamide. Interestingly, benzamide was selectively produced, even though the conditions (KOH in ethanol–water mixture) tended to produce carboxylic acids.[3] The reaction appeared to stall at the intermediate stage (benzamide) due to the steric hindrance of the trifluoromethyl group. Under the same conditions, 4-dodecyloxybenzoic acid was produced from 4-dodecyloxybenzonitrile. 4-Dodecyloxybenzamide was produced by using sodium percarbonate, which selectively generates aromatic primary amides in the absence of a substituent at the *ortho* position.[49] The resulting compound was much less soluble than 4-dodecyloxy-2-trifluoromethylbenzamide in most solvents, and it easily crystallized. Two polymorphic forms of 4-dodecyloxy-2-trifluoromethylbenzamide have been identified: crystals grown from hexanes or formed from a melt share one polymorphic form (**L** polymorph) determined by X-ray crystallography. The resolved crystal structure is shown in Fig. 9a. A two-dimensional hydrogen bonded network of benzamide was observed, as expected. The length of the N–H···O bond was calculated to be 3.0 Å for face-to-face hydrogen bonds and 2.8 Å for side-to-side hydrogen bonds. The observation of short side-to-side hydrogen bonds relative to the face-to-face bonds was unusual for benzamide. Similar two-dimensional hydrogen bonding was observed in an analogous compound, 4-hexylbenzamide; however, the length of the N–H···O face-to-face hydrogen bond was short (2.9 and 3.0 Å).[50] The trifluoromethyl group near the carbonyl oxygen apparently disrupted the optimal geometry for the face-to-face hydrogen bonding. The dihedral angle between the aromatic plane and the plane composed of non-H atoms in the amide was 53° in 4-dodecyloxy-2-trifluoromethylbenzamide, indicating significant tilting (compared to 29.3° in 4-hexylbenzamide) due to the presence of the trifluoromethyl group. The distance between the aromatic rings was 4.0 Å. Two types of conformational isomer were observed, depending on the position of the fluorine atoms, even though one isomer was dominant (95 : 5 ratio). The alkyl chain configuration was all-*trans* and was fully intercalated, suggesting that the presence of van der Waals interactions between the alkyl chains provided a driving force for crystallization.

Crystallization of the compound in other solvents, such as ethanol, yielded a different polymorphic form (**S** polymorph), identified by powder X-ray diffraction studies. Although significant structural differences were apparent, it was not possible to grow a crystal suitable for single crystal X-ray diffraction studies. The position of the primary diffraction peak in the diffractogram appeared at $d$ = 1.48 nm, which was much smaller than in the **L** polymorphic form ($d$ = 2.39 nm). Significant disorder and a high population of the *gauche* conformation in the alkyl chain was suggested and was supported by FT-IR and DSC studies. The FT-IR spectra revealed a large red shift in the symmetric N–H stretching compared to the **L** polymorphic form, suggesting the presence of stronger hydrogen bonding. This evidence suggested that the **S** polymorphic form was stabilized by strong face-to-face hydrogen bonding. In contrast to conventional 2-substituted benzamides, $H_{anti}$ was thought to point toward the trifluoromethyl substituent *via* intramolecular hydrogen bonding with one of the fluorine atoms in the trifluoromethyl group. In this configuration the carbonyl oxygen would have a less sterically crowded environment than that of **L** polymorphic form and form stronger face-to-face hydrogen bonding with $H_{syn}$. $H_{anti}$ would also form side-to-side hydrogen bonding with the neighboring carbonyl oxygen in addition to intramolecular hydrogen bonding. Poorly packed alkyl chains may have been the cost of forming stronger hydrogen bonds.

The ability to form two different polymorphs was tested by dissolving 4-dodecyloxy-2-trifluoromethylbenzamide in hot ethanol, which was then cast onto a Si wafer (Fig. 10a–b). After rapid evaporation of the ethanol, three-dimensional rectangular macroporous structures were observed on the surface with a cross-section of *ca*. 10 × 20 μm. Indeed, both polymorphic forms were obtained after evaporation, with a higher population

 

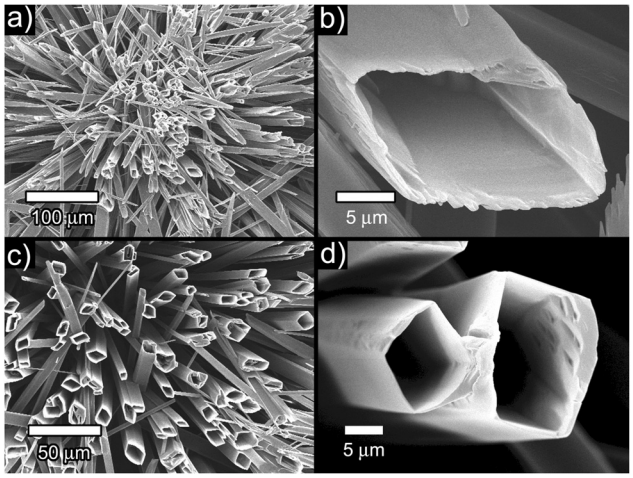


**Fig. 10** Drying mediated self-assembly of 2-substituted aromatic primary amides: SEM images of macroscopic parallelogrammatic pipes. (a) A macroscopic view of the hemispherically formed pipes, and (b) an enlarged view of a typical pipe of 4-dodecyloxy-2-trifluoromethylbenzamide. Reprinted from ref. 48 with permission from Wiley-VCH. (c) A macroscopic view of the hemispherically formed pipes, and (d) an enlarged view of a typical pipe of 4-tetradecyloxy-2-trifluoromethylbenzamide. Reprinted from ref. 51 with permission from Wiley-VCH.

of the **L** polymorph. A time-dependent structural study indicated that the solvent-rich **S** polymorph formed in ethanol first, then transformed into the **L** form by rapid crystallization at the solution–air interface. Under evaporation, the assembly process was expected to be dynamic but irreversible. Flow of the solute toward the interface and consumption by crystallization eventually left solvent on the inner walls of the **L** polymorph, the macroscopic shape of which resembled that of the **S** polymorph, thereby generating hollow-edged macroscopic objects. A subsequent study of a series of analogs with different alkyl chain lengths revealed that longer alkyl chain derivatives crystallized faster into three-dimensional structures and preferred the **L** polymorphs to the **S** forms due to increased contributions of van der Waals interactions among the alkyl chains (Fig. 10c–d).[51] However, under strong van der Waals forces, a macroscopic pipe structure was not observed, because the structure could not undergo a polymorphic transition.

### Dendritic organogelators: nanofibers

Although the 4-dodecyloxy-2-trifluoromethylbenzamide revealed an interesting self-assembled structure in the solid state, the compound exhibited a strong tendency to crystallize instead of forming a thermotropic liquid crystalline phase or nanostructures in solution. This led to the idea of introducing a dendritic branch into the molecule and synthesizing a Fréchet-type benzyl ether dendron with aromatic primary amides at the periphery. This molecular design enabled the introduction of spatial asymmetry originating from the wedge shape, which could potentially reduce the crystallinity of the aromatic primary amide motif. More importantly, the number of amides at the periphery could be controlled by the generation of the dendron, which allowed investigation of multivalent noncovalent interactions among the amides. Fig. 11a shows the structures of the primary amide-containing dendrons employed in the study.[52] Several bis-dendritic structures comprising amide dendrons and alkyl dendrons of different generations were compared to investigate the multivalent interactions among the amides and the balance among the noncovalent interactions. A molecule containing a first-generation amide dendron and a first-generation alkyl dendron (**G1-G1**) formed a physical gel over a wide range of solvents by forming a three-dimensional self-assembled fibrillar network, whereas the unbalanced **G1-G0** and **G0-G1** formed gels in fewer solvents. The **G1-G0** derivative without trifluoromethyl groups was poorly soluble in common organic solvents and mostly precipitated out of solution during cooling, not forming a gel. **G2-G0** was also barely soluble and formed poorly structured aggregates. The number of amides determined the strength of hydrogen bonding; however, balance among the dendrons significantly affected the self-assembly process by adjusting the strength of the hydrogen bonds and the van der Waals interactions. Concentration-dependent NMR experiments showed that **G1**-containing molecules exhibited higher association constants and formed large aggregates in solution relative to the **G0**-containing molecules, which formed dimers, demonstrating the importance of multivalent cooperative interactions among amides at the periphery.

This approach to the fabrication of hierarchically structured organic materials was extended by synthesizing a photopolymerizable version of **G1-G1** that included diacetylene moieties in the alkyl chain (**G1-GDA**, **17**) (Fig. 12a).[53] **G1-GDA** showed gelation behavior similar to **G1-G1**, whereas fascinating honeycomb patterns could be generated when a chloroform solution of **G1-GDA** was cast in a flow of moist air (Fig. 12b–c). "Breath-figured" honeycomb structures are usually observed in polymer solutions in which a viscous polymer solution undergoes solidification around condensing water droplets. Self-assembled **G1-GDA** nanofibers in solution were thought to behave similarly to polymer chains, which stabilize water droplets and prevent them from coalescing. The photopolymerizable diacetylene moieties permitted lithographic patterning of the self-assembled honeycomb structure, demonstrating the strength of this combination of top-down and bottom-up approaches (Fig. 12d–e).

### Noncovalently crosslinked polymeric nanoparticles

Hydrogen bonding between primary amides in the polymeric systems was exemplified by poly(*N*-acryloyl glycinamide), a water-soluble polymer bearing a primary amide motif in each repeating unit.[54] The polymer formed thermoreversible gels in concentrated aqueous solutions due to the physical crosslinking *via* randomly distributed hydrogen bonds of primary amides.[55] The polymer solution also exhibited upper critical solution temperature behavior based on thermally reversible hydrogen bonding.[56] Poly(styrene-$d_8$-*co*-4-vinylbenzamide) has been used to strengthen the interface between immiscible polystyrene and poly(2-vinylpyridine) *via* interactions between the benzamide and the pyridine moieties.[57] The benzamide was found to be less useful than the phenol group, which is a stronger hydrogen bond donor and provides a better match to

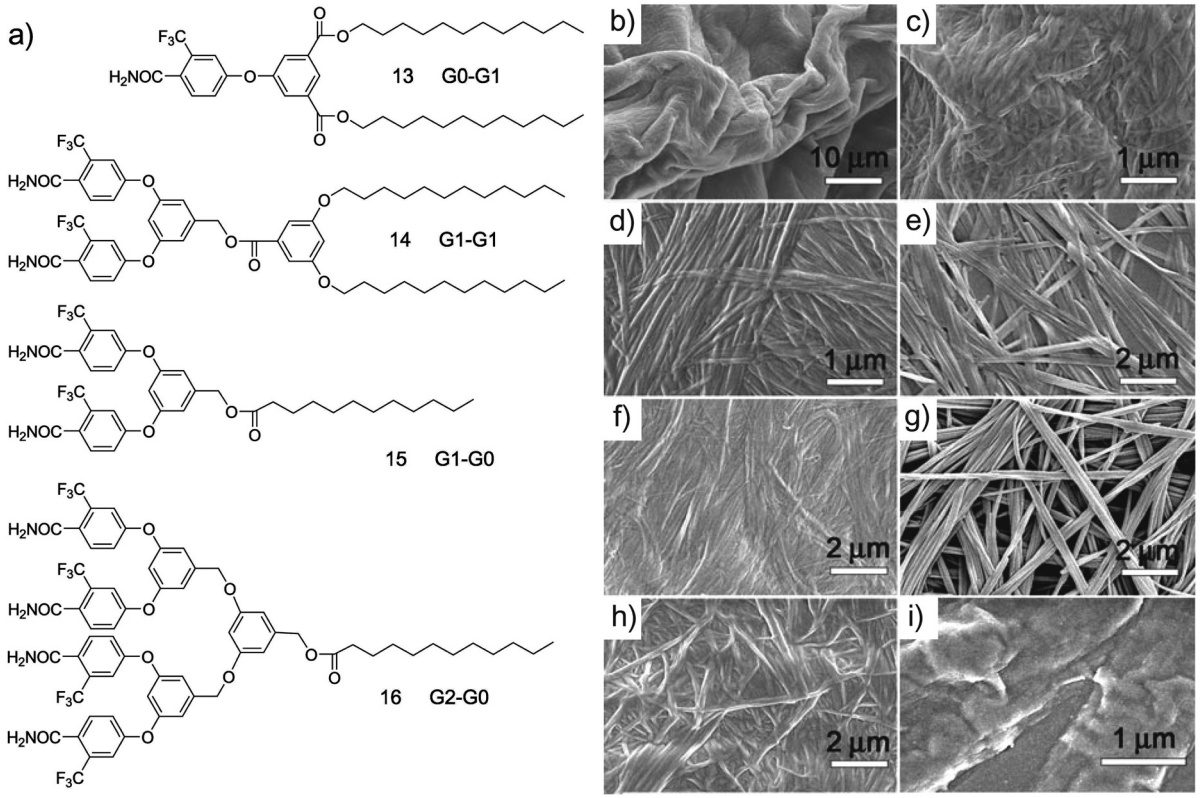


**Fig. 11** Self-assembly of the aromatic primary amides in dendrons. (a) Chemical structures of bis-dendritic gelators consisting of benzamide dendrons and alkyl dendrons. SEM images of the xerogel of (b,c) **G1-G0** from toluene, (d) **G1-G0** from xylene, (e) **G1-G1** from benzene, (f) **G1-G1** from toluene, (g) **G1-G1** from 1-butanol, and (h) **G0-G1** from hexane. (i) SEM image of the solid of **G2-G0** obtained by evaporation of a solution drop of chlorobenenzene on a Si wafer. Reprinted from ref. 52 with permission from Wiley-VCH.

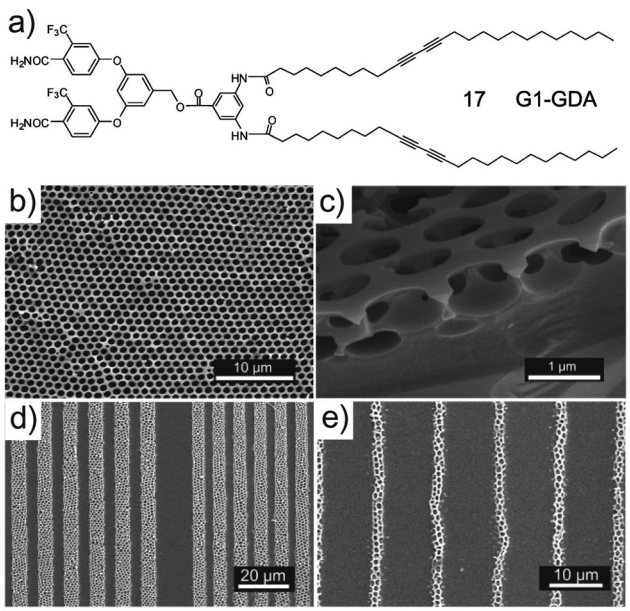


**Fig. 12** Hierarchically self-assembled structures from photopolymerizable dendritic organogelator. (a) Chemical structure of bis-dendritic gelator **17** (**G1-GDA**) consisting of a benzamide dendron and an alkyl dendron including diacetylene moieties. (b,c) SEM images of the honeycomb structure of **17** formed by the breathe-figure technique. (d,e) SEM images of the patterned honeycomb lines after exposing to deep UV irradiation (220–260 nm) using a line-patterned photomask. Reprinted from ref. 53 with permission from Wiley-VCH.

pyridine. We once again decided to take advantage of self-complementary hydrogen bonded networks of primary amides in the construction of noncovalently crosslinked polymeric nanoparticles (Fig. 13).[58] A methacrylic monomer consisting of first-generation dendritic primary amides was synthesized and copolymerized with methyl methacrylate *via* the reversible addition-fragmentation chain transfer (RAFT) polymerization method. Thanks to the high tolerance of RAFT to a variety of functional monomers, well-defined copolymers with various amounts of hydrogen bonding monomers were obtained. The polymer with 6.1 mol% hydrogen bonding monomers was self-assembled in toluene by dissolving the polymer in a mixture of tetrahydrofuran (THF) and toluene, followed by evaporation of the more volatile THF. Hydrogen bonding was facilitated in toluene, and nanoparticles formed by intramolecular "collapse" of the chain *via* multivalent cooperative hydrogen bonding and solubilization of the PMMA backbone. Dynamic light scattering and SFM experiments revealed uniform nanoparticles 24 nm in diameter, suggesting a low aggregation number for the polymer chains (Fig. 13b–c). Viscosity measurements clearly demonstrated that the polymer chains underwent a conformational change from coils in THF to particles in toluene, as indicated by the substantial drop in the viscosity. A reference polymer copolymerized with a dendritic monomer that did not form hydrogen bonds did not show any changes in the viscosity.

 

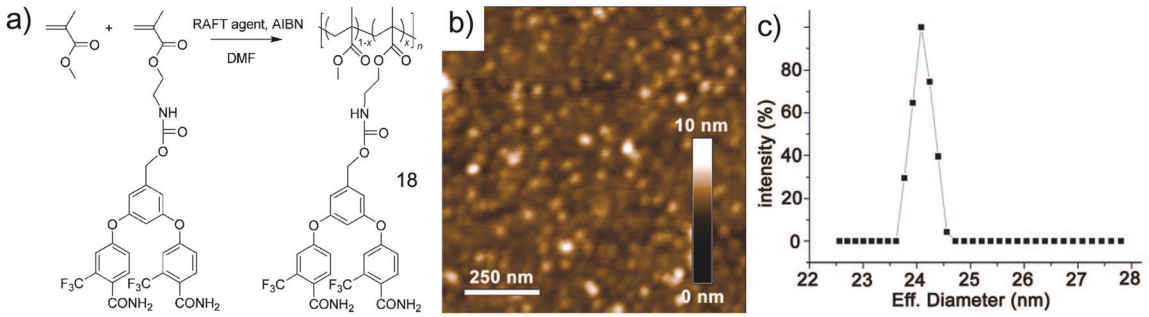


**Fig. 13** Self-assembly of the aromatic primary amides in polymers. (a) Synthesis of copolymers **18** containing first-generation benzamide-dendrons (6.1 mol%). (b) SFM image of nanoparticles of **18** prepared in toluene on a Si wafer. (c) DLS plot of nanoparticles of **18** prepared in toluene. Reprinted from ref. 58 with permission from American Chemical Society.



## Conclusions and outlook

Hydrogen bonding among primary amides has produced interesting self-assembled structures based on the unique two-dimensional hydrogen bonded networks of amides in conjunction with other noncovalent interactions. The use of primary amides, for example, their application to self-assembled structures beyond crystal engineering, has been limited presumably due to the tendency of amides to form crystals. In addition to elaborating previous strategies, such as introducing amides at the focal points of bulky dendrons or combining amides with conjugated aromatics, we successfully introduced the 2-trifluoromethyl benzamide motif into several classes of molecule ranging from small molecules to dendrimers and polymers and demonstrated that diverse self-assembled structures could be generated. We believe the 2-trifluoromethyl benzamide motif will find use as a reliable supramolecular synthon in the design of self-assembled materials. By choosing an appropriate functional molecular segment and conjugating with the 2-trifluoromethyl benzamide-containing "module" that forms a desired self-assembled structure, functional self-assembled structures will be generated and find applications such as chiral self-assembled materials, supramolecular electronics, self-healing supramolecular polymer networks. Along with efforts to utilize primary aromatic amides for applications, further studies should pursue more sophisticated control of the hydrogen bonding by introducing different substituents in the aromatic ring not only to tune steric and electronic environments but also to guide the direction of hydrogen bonding. Combination of primary aromatic amides with other hydrogen bonding motifs will be also an interesting direction for generation of more complicated self-assembled materials as witnessed in crystal engineering.[59] Deeper understanding of the hydrogen bonding of the primary aromatic amides will make the toolset of supramolecular chemistry even richer.

## Acknowledgements

The authors are grateful to the National Research Foundation (NRF) through NRL (R0A-2008-000-20121-0) program and the Ministry of Environment through Contract No. 20090192091001-B0-0-001-0-0-2009.

## References

1 S. S. Kuduva, D. Bläser, R. Boese and G. R. Desiraju, *J. Org. Chem.*, 2001, **66**, 1621–1626.
2 A. Greenberg, C. M. Breneman and J. F. Liebman, *The Amide Linkage: Structural Significance in Chemistry, Biochemistry, and Materials Science, Wiley-IEEE*, 2002.
3 M. B. Smith and J. March, *March's Advanced Organic Chemistry: Reactions, Mechanisms, and Structure*, Wiley, 6th edn, 2007.
4 J. N. Moorthy and N. Singhal, *J. Org. Chem.*, 2005, **70**, 1926–1929.
5 V. Y. Kukushkin and A. J. L. Pombeiro, *Chem. Rev.*, 2002, **102**, 1771–1802.
6 M. A. Bennett and T. Yoshida, *J. Am. Chem. Soc.*, 1973, **95**, 3030–3031.
7 E. S. Kim, H. S. Lee, S. H. Kim and J. N. Kim, *Tetrahedron Lett.*, 2010, **51**, 1589–1591.
8 H. Fujiwara, Y. Ogasawara, K. Yamaguchi and N. Mizuno, *Angew. Chem., Int. Ed.*, 2007, **46**, 5202–5205.
9 J. F. Hull, S. T. Hilton and R. H. Crabtree, *Inorg. Chim. Acta*, 2010, **363**, 1243–1245.
10 C. L. Allen, C. Burel and J. M. J. Williams, *Tetrahedron Lett.*, 2010, **51**, 2724–2726.
11 L. Cao, J. Ding, M. Gao, Z. Wang, J. Li and A. Wu, *Org. Lett.*, 2009, **11**, 3810–3813.
12 A. Khalafi-Nezhad, B. Mokhtari and M. N. S. Rad, *Tetrahedron Lett.*, 2003, **44**, 7325–7328.
13 C. L. Allen and J. M. J. Williams, *Chem. Soc. Rev.*, 2011, **40**, 3405–3415.
14 J. W. Kim, K. Yamaguchi and N. Mizuno, *Angew. Chem., Int. Ed.*, 2008, **47**, 9249–9251.
15 X.-F. Wu, H. Neumann and M. Beller, *Chem.–Eur. J.*, 2010, **16**, 9750–9753.
16 M. C. Etter, *Acc. Chem. Res.*, 1990, **23**, 120–126.
17 L. Leiserowitz and G. M. J. Schmidt, *J. Chem. Soc. A*, 1969, 2372–2382.
18 C. B. Aakeröy, B. M. T. Scott and J. Desper, *New J. Chem.*, 2007, **31**, 2044–2051.
19 Z. Berkovitch-Yellin and L. Leiserowitz, *J. Am. Chem. Soc.*, 1980, **102**, 7677–7690.
20 L. Shimoni, J. P. Glusker and C. W. Bock, *J. Phys. Chem.*, 1996, **100**, 2957–2967.
21 C. M. Reddy, L. S. Reddy, S. Aitipamula, A. Nangia, C.-K. Lam and T. C. W. Mak, *CrystEngComm*, 2005, **7**, 44–52.
22 J. Liebig and F. Wöhler, *Ann. Pharm.*, 1832, **3**, 249–282.
23 W. I. F. David, K. Shankland, C. R. Pulham, N. Blagden, R. J. Davey and M. Song, *Angew. Chem., Int. Ed.*, 2005, **44**, 7032–7035.
24 J. Thun, L. Seyfarth, J. Senker, R. E. Dinnebier and J. Breu, *Angew. Chem., Int. Ed.*, 2007, **46**, 6729–6731.
25 R. K. Kumar, S. Balasubramanian and I. Goldberg, *Chem. Commun.*, 1998, 1435–1436.
26 S. A. Baudron, N. Avarvari, P. Batail, C. Coulon, R. Clérac, E. Canadell and P. Auban-Senzier, *J. Am. Chem. Soc.*, 2003, **125**, 11583–11590.
27 P. Holý, P. Sehnal, M. Tichý, J. Závada and I. Císařová, *Tetrahedron: Asymmetry*, 2003, **14**, 245–253.
28 K. Kobayashi, A. Sato, S. Sakamoto and K. Yamaguchi, *J. Am. Chem. Soc.*, 2003, **125**, 3035–3045.

29 S. Ahn, C. N. Morrison and A. J. Matzger, *J. Am. Chem. Soc.*, 2009, **131**, 7946–7947.
30 S. Ahn and A. J. Matzger, *J. Am. Chem. Soc.*, 2010, **132**, 11364–11371.
31 R. Plehnert, J. A. Schröter and C. Tschierske, *J. Mater. Chem.*, 1998, **8**, 2611–2626.
32 C. Tan, L. Su, R. Lu, P. Xue, C. Bao, X. Liu and Y. Zhao, *J. Mol. Liq.*, 2006, **124**, 32–36.
33 V. Percec, W.-D. Cho, G. Ungar and D. J. P. Yeardley, *Angew. Chem., Int. Ed.*, 2000, **39**, 1597–1602.
34 U. Beginn and G. Lattermann, *Mol. Cryst. Liq. Cryst.*, 1994, **241**, 215–219.
35 V. Percec, J. Smidrkal, M. Peterca, C. M. Mitchell, S. Nummelin, A. E. Dulcey, M. J. Sienkowska and P. A. Heiney, *Chem.–Eur. J.*, 2007, **13**, 3989–4007.
36 M. Lehmann, C. Köhn, H. Meier, S. Renker and A. Oehlhof, *J. Mater. Chem.*, 2006, **16**, 441–451.
37 W. W. Bates and M. E. Hobbs, *J. Am. Chem. Soc.*, 1951, **73**, 2151–2156.
38 M. E. Hobbs and W. W. Bates, *J. Am. Chem. Soc.*, 1952, **74**, 746–749.
39 P. J. Krueger and D. W. Smith, *Can. J. Chem.*, 1967, **45**, 1611–1618.
40 U. Beginn, S. Sheiko and M. Möller, *Macromol. Chem. Phys.*, 2000, **201**, 1008–1015.
41 L. A. Estroff and A. D. Hamilton, *Chem. Rev.*, 2004, **104**, 1201–1217.
42 X. Yang, R. Lu, T. Xu, P. Xue, X. Liu and Y. Zhao, *Chem. Commun.*, 2008, 453–455.
43 X. Yang, R. Lu, P. Xue, B. Li, D. Xu, T. Xu and Y. Zhao, *Langmuir*, 2008, **24**, 13730–13735.
44 X. Yang, R. Lu, H. Zhou, P. Xue, F. Wang, P. Chen and Y. Zhao, *J. Colloid Interface Sci.*, 2009, **339**, 527–532.
45 Z. Berkovitch-Yellin, J. van-Mil, L. Addadi, M. Idelson, M. Lahav and L. Leiserowitz, *J. Am. Chem. Soc.*, 1985, **107**, 3111–3122.
46 P. Campomanes, M. I. Menéndez and T. L. Sordo, *J. Phys. Chem. A*, 2002, **106**, 2623–2628.
47 A. N. Chekhlov, *J. Struct. Chem.*, 2002, **43**, 338–345.
48 M. Seo, G. Seo and S. Y. Kim, *Angew. Chem., Int. Ed.*, 2006, **45**, 6306–6310.
49 G. W. Kabalka, S. M. Deshpande, P. P. Wadgaonkar and N. Chatla, *Synth. Commun.*, 1990, **20**, 1445–1451.
50 H. C. Kwong, M. Z. Ab Rahman, M. I. M. Tahir and S. Silong, *Acta Crystallogr., Sect. E: Struct. Rep. Online*, 2011, **E67**, O612.
51 M. Seo, J. H. Kim, G. Seo, C.-H. Shin and S. Y. Kim, *Chem.–Eur. J.*, 2009, **15**, 612–622.
52 M. Seo, J. H. Kim, J. Kim, N. Park, J. Park and S. Y. Kim, *Chem.–Eur. J.*, 2010, **16**, 2427–2441.
53 J. H. Kim, M. Seo and S. Y. Kim, *Adv. Mater.*, 2009, **21**, 4130–4133.
54 H. C. Haas and N. W. Schuler, *J. Polym. Sci., Polym. Lett. Ed.*, 1964, **2**, 1095–1096.
55 H. C. Haas, M. J. Manning and M. H. Mach, *J. Polym. Sci., Part A1*, 1970, **8**, 1725–1730.
56 J. Seuring, F. M. Bayer, K. Huber and S. Agarwal, *Macromolecules*, 2012, **45**, 374–384.
57 B. D. Edgecombe, J. M. J. Fréchet, Z. Xu and E. J. Kramer, *Chem. Mater.*, 1998, **10**, 994–1002.
58 M. Seo, B. J. Beck, J. M. J. Paulusse, C. J. Hawker and S. Y. Kim, *Macromolecules*, 2008, **41**, 6413–6418.
59 Ö. Almarsson and M. J. Zaworotko, *Chem. Commun.*, 2004, 1889–1896.




 